JASA ARTICLE

An easy to implement empirical approach for estimating underwater sound transmission loss during pile driving in Florida

Raphael Crowley,[1,a)] Moses Bosco,[1] Amanda Schaaf,[2] Mariam Makoleo,[1] Consolatha Mushi,[1] Brandon Rivera,[1] Jonathan Berube,[1] Clark Morgan,[2,b)] Emily Sapp,[2] Christian H. Matemu,[3] Dillon Sypula,[1] James J. Gelsleichter,[2] and Brian T. Kopp[4]

[1]*School of Engineering, University of North Florida, Jacksonville, Florida 32224, USA*

[2]*Department of Biology, University of North Florida, Jacksonville, Florida 32224, USA*

[3]*Department of Civil and Coastal Engineering, Engineering School of Sustainable Infrastructure and the Environment, University of Florida, Gainesville, Florida 32611, USA*

[4]*Engineering Department, Jacksonville University, Jacksonville, Florida 32211, USA*

ABSTRACT:

Underwater noise data were collected from 84 pile drives during bridge construction at various sites in Florida. These data were used to develop an empirically based model for underwater transmission loss associated with root mean squared, peak, and sound exposure level values. The model was verified using readings from other datasets as well as data from this study, and it appeared to reproduce reported transmission loss coefficient values well when data were curated to match data used in the empirical model's development and limited to situations where robust data were used in model development. As such, the model described here has some limitations, but in the context of pile driving in Florida where most piles are of similar dimensions and driven in similar water depths, especially during impact pile driving concrete piles, it may represent a useful design tool that engineers can use to predict underwater noise due to pile driving without the need to sample sound at multiple locations during driving.

 https://doi.org/10.1121/10.0034619

(Received 19 March 2024; revised 18 November 2024; accepted 21 November 2024; published online 17 December 2024)

[Editor: Kay L. Gemba] Pages: 4048–4060

I. INTRODUCTION

A. Background information

In recent years, several federal agencies have expressed concerns about the effects of underwater pile driving activities on marine organisms. In particular, there is concern that underwater pile driving activities may exceed certain noise thresholds that are known to cause physical injury, adverse behavior, or death for fish and other marine taxa. These thresholds have been investigated by several authors in the literature (Finneran *et al.*, 2011; Buehler *et al.*, 2015; Finneran, 2015; Tougaard *et al.*, 2015; Erbe *et al.*, 2016; Lucke *et al.*, 2016; Kastelein *et al.*, 2017; Popper and Hawkins, 2019).

While the thresholds that may cause injury to marine wildlife are becoming better understood, the distance from a pile where these thresholds are exceeded has, until recently, been very poorly characterized. Over the past 15 years, several authors have studied underwater sound propagation during pile driving. As discussed by Martin and Barclay (2019), often these studies occur during the installation of wind farms (Bailey *et al.*, 2010; Brandt *et al.*, 2011; Dähne *et al.*, 2013). More generally, several other studies have also emerged that improve overall understanding associated with underwater anthropogenic sound propagation (Reinhall and Dahl, 2011a,b; Dahl and Reinhall, 2013; Ainslie *et al.*, 2014; Lippert and von Estorff, 2014; Dahl *et al.*, 2015; Lippert *et al.*, 2015; Reinhall *et al.*, 2015; Dahl and Dall'Osto, 2017; Wilkes and Gavrilov, 2017; Lippert *et al.*, 2018; Jestel *et al.*, 2021; von Pein *et al.*, 2022). Common to most of these studies is that the authors usually attempt to quantify underwater transmission loss (TL), which is defined as

$$\mathrm{TL} = L_s - L_r, \tag{1}$$

where L_s is the sound pressure level (SPL) in decibels (dB) at the source (i.e., the pile) and L_r is the SPL at some range (i.e., distance from the pile), r. SPL is further defined as

$$\mathrm{SPL\,(dB)} = 10\log_{10}\frac{p^2}{p_0^2}, \tag{2}$$

in which p is the sound pressure and p_0 is the reference pressure, which was taken to be 1 μPa throughout this article.

[a)]Email: r.crowley@unf.edu

[b)]Present address: Harbor Branch Oceanographic Institute, Florida Atlantic University, 5600 North U.S. Highway 1, Fort Pierce, FL 34946, USA.

https://doi.org/10.1121/10.0034619

From a design perspective, the determination of TL has remained a challenge due to a number of factors discussed in depth by Ainslie *et al.* (2014). Most TL models through fluid media assume point or dipole sound sources. However, a pile drive is neither because the pile spans the entire water column. In addition, current TL models usually assume a uniform medium, but in the case of the pile drive, this is not true either because sound propagates through the air, water, and soil. Some have attempted to take these variable sound media conditions into account using more sophisticated models for sound propagation in shallow water—examples include Rogers (1981), and Kaczkowski (2010), although there are many others. However, these models often require calibration of several variables that are difficult to measure during construction operations such as sound speed through soil, variable soil densities, etc.

In the absence of a sophisticated, easy-to-use model that describes underwater TL well, state and federal agencies have used the Practical Spreading Loss model described by several authors including Buehler *et al.* (2015) and NOAA (2021),

$$\mathrm{TL} = 15\log_{10}\left(\frac{r}{r_0}\right). \tag{3}$$

This model represents the logarithmic halfway point between cylindrical and spherical spreading that assumes TL is mostly due to mode stripping. As pointed out by Weston (1971), Ainslie (2010), and Ainslie *et al.* (2014), Eq. (3) is derived from the exact solution for cylindrical spreading for a point source far from a boundary at frequencies above the cutoff frequency. The exact solution to this situation is

$$\mathrm{TL} = 15\log_{10}\left(\frac{r}{r_0}\right) + 5\log_{10}\left(\frac{\eta H}{\pi r_0}\right)^{1/2}, \tag{4}$$

where H is the water depth. Ainslie *et al.* (2014) point out that Eq. (3) is simply a special case of Eq. (4) where A is assumed to equal zero which implies that $\eta H = \pi r_0$. More generally then, the full equation for underwater TL is

$$\mathrm{TL} = A\log_{10}\left(\frac{r}{r_0}\right) + B. \tag{5}$$

In the case of Eq. (4), $B = 5\log_{10}(\eta H/\pi r_0)^{1/2}$ while $A = 15$ (Ainslie *et al.*, 2014).

Ainslie *et al.* (2014) go on to provide several other examples where A and B from Eq. (5) are computed for situations other than point sources far from boundaries above the cutoff frequency including transient and dipole sources. In each solution, some value of A from Eq. (5) is derived along with a term or terms that comprise B. These solutions imply that A and B must be co-dependent and interrelated. More recently, Lippert *et al.* (2018) provided an analytical solution of the form of Eq. (5) that accounted for the line-source associated with a pile drive,

$$\mathrm{TL} = 10\log_{10}\left(\frac{r}{r_0}\right) + \alpha(r - r_0), \tag{6}$$

where α is a decay factor given by

$$\alpha = \frac{\left(-10\log_{10}\left(|R|^2\right)\right)}{2H\cot(\theta) + \Delta l}. \tag{7}$$

In Eq. (7), R is a power reflection coefficient defined by the squared magnitude of the reflection factor between water and soil; θ is the angle from which sound leaves the pile derived from the ratio between sound speed through the pile and sound speed in water—see Reinhall and Dahl (2011b) for details; Δl is the horizontal beam shift described in detail by Weston (1994); and H is the water depth. Martin and Barclay (2019) pointed out that Eq. (6) may be further generalized,

$$L_r = C - A\log_{10}\left(\frac{r}{r_0}\right) + B(r - r_0). \tag{8}$$

In Eq. (8), L_s has been replaced by a constant, C, that is not necessarily a source term, but rather, according to Martin and Barclay (2019) depends on project-specific conditions such as strike energy (SE), the coupling of hammer energy into the pile, and the damping of pile vibrations by the sediment (see Lippert *et al.*, 2016; MacGillivray, 2013, for additional details). The B-term in Eq. (8) is due to multiple reflections between the seabed and surface while the A-term is due to bottom composition, the water-column sound speed profile, surface roughness, and seabed roughness. Martin and Barclay (2019) go on to present their own model that is a function of SE; pile penetration (PP), and the angle between the pile and the receiver, θ,

$$\begin{aligned} TL &= L_s - L_r \\ &= \left[10\log_{10}\frac{r}{r_0} + \alpha\frac{r}{r_0}\right] \\ &\quad - \left[\mathrm{ASE} + B\mathrm{PP} + C\left(\frac{r}{r_0}\right) + D\cos\theta + E\left(\frac{r}{r_0}, \cos\theta\right)\right]. \end{aligned} \tag{9}$$

In Eq. (9), α was found to be frequency dependent. In this equation, attenuation terms are separated from source terms or pseudo-source terms by brackets.

The Martin and Barclay (2019) and Lippert *et al.* (2018) studies both represent breakthrough leaps in terms of overall understanding of the anthropogenic sound transmission due to pile driving. However, while Lippert *et al.* (2018) provide a physically-based approach for determining underwater transmission loss, the authors reported that field testing with their model [i.e., Eq. (6) and Eq. (7)] showed that errors may be as high as 33%. To improve upon this, presumably, one could utilize Eq. (8), but this would require calibration of the A, B, and C coefficients from Eq. (8). The Martin and Barclay (2019) model [i.e., Eq. (9)] has a similar

issue in the sense that it requires calibration of the A, B, C, D, and E coefficients from Eq. (9). Martin and Barclay (2019) recommended logarithmically spacing at least four hydrophones during pile driving operations to perform this calibration.

B. Goals and objectives

The goal of the work presented herein was to simplify the approaches presented by Martin and Barclay (2019) and Lippert *et al.* (2018) and develop a simple, easy-to-implement model for predicting underwater TL that requires no calibration. In particular, the authors of this study sought to take advantage of the interdependency between A and B from Eq. (5) which was discussed in depth by Ainslie *et al.* (2014).

As noted previously, the current standard for estimating underwater transmission loss during pile driving during construction projects is the National Marine and Fisheries Services (NMFS) calculator (NOAA, 2021). This model utilizes Eq. (3) to estimate TL and presumes that SPL is known at one location during pile driving. Thus, investigators took a similar approach throughout this study in the sense that it was assumed that like NOAA (2021), SPL was known at one location during pile driving operations.

II. METHODOLOGY

A. Site information

The first step in the development of a new, empirically based underwater sound propagation model that could be used during pile driving operations was to collect field data. Significant data have already been collected during underwater pile driving operations; Buehler *et al.* (2015) summarize these data well. However, most of these data came from California and Washington State during steel pile drives, and it was unclear how these data would translate to geotechnical conditions typical in Florida or typical Florida bridge pile drives where concrete (as opposed to steel) piles are typically installed. As a result, data were collected from several underwater pile driving sites in Florida as summarized in Table I. Note that the reason these piles were selected was simply because these were the transportation-related locations in the State of Florida where underwater pile driving happened to be occurring between 2018 and 2023.

B. Data collection

1. Data collection system

Data were collected using a system of buoy-mounted hydrophones described in detail by Crowley *et al.* (2020). To summarize, hydrophones were suspended from floating platform systems that consisted of two small pontoons attached to aluminum frames. Each frame held a Pelican™ 1450 box that housed the electronics for the system. Scanstrut cable clam/deck seals were used to pass a hydrophone cable and a thermocouple cable from the exterior into the box while a MENCOM MDE45-8FR-RJ45-BM waterproof Ethernet connection was used to route an Ethernet cable into the case. Electronics in the cases consisted of Bruel and Kjaer 2250 handheld analyzers; Bruel & Kjaer 2647 charge converters (Bruel & Kjaer, Naerum, Denmark); L-Com BT-CAT5-P1 power-over-Ethernet converters (L-Com, North Andover, MA); 24-volt motorcycle batteries connected in series. Outside of each box were a Bruel & Kjaer 8103 hydrophone; a Ubiquiti Bullet M2 wireless access point; and an L-COM HG2409UP antenna. The batteries, power converter, Bullet, and antenna connect to the handheld analyzer via Ethernet cable and broadcast the measured sound data to a computer in real-time. In addition, Garmin GPSMAP (Garmin, Olathe, KS) global position system (GPS) units were added to each box to track the buoys' geolocations. Hydrophone cables were attached to wire strain relief systems to protect the instruments. In total, five of these floating data collection systems were built so that data from five ranges from the piles could be captured

TABLE I. Pile driving site information (note that PCP stands for prestressed concrete pile).

Site Name	Northing	Easting	Pile Dim. (cm)	Pile Length (m)	Pile Type	Hammer Type	No. Drive
Bayway E	27°41′36.44"	82°43′4.5"	91 × 91	26	Square PCP	200T vibratory	1
Dunn's Creek	29°34′39.2″	81°37′34.0″	46 (width)	Varied	Sheet	200T vibratory	2
Ribault River	30°23′37.4″	81°42′48.2″	61 × 61	33.5	Square PCP	APE D96-42	4
Suwannee River	30°14′40.9″	83°15′0.3″	61 (diam)	Varied	Open Steel	Del-Mag D-46	3
County Road (CR) 218	30°3′37.8″	81°52′17.8″	61 × 61	33.5	Square PCP	APE D46-32	3
State Road (SR) 23	30°4′19.0″	81°49′8.0″	61 × 61	29	Square PCP	APE D62	9
Choctawhatchee Bay	30°24′49.0″	86°9′44.4″	46 (width)	Varied	Sheet	200T vibratory	2
Howard Frankland (West)	27°55′48.2″	82°34′55.4″	76 × 76	22.3	Square PCP	APE D80-42	18
Howard Frankland King Piles	27°55′48.2″	82°34′55.4″	99 × 30	∼15	W 40 × 183	APE D80-42	9
Howard Frankland (East)	27°55′48.2″	82°34′55.4″	76 × 76	22.3	Square PCP	APE D80-42	15
Simpson's Creek	30°27′17.8″	81°27′53.5″	61 × 61	21	Square PCP	APE D36-32	1
Loxahatchee River	26°56′50.2″	80°5′24.6″	76 × 76	40	Square PCP	Pileco D100-13	4
Manatee River	27°39'57.8"	82°25'58.1″	61 × 61	29	Square PCP	APE D62-52	3
NASA Causeway	28°31′38.9″	80°45′25.8″	76 × 76	40	Square PCP	Pileco D70-32	9
Broward River	30°26′14.7"	81°38′32.8"	61 × 61	22	Square PCP	APE D-50 OED	1

https://doi.org/10.1121/10.0034619

simultaneously. Prior to each buoy deployment, buoy hydrophones were calibrated using a Bruel & Kjaer type 4229 calibrator.

2. Data collection procedure

Buoys were deployed at bridge locations at varying distances from piles and anchored using river anchors. In general, investigators tried to get the first buoy as close to a pile or pile bent as possible while maintaining safety. Once the first buoy was deployed a "double-the-distance" rule of thumb was used to position the subsequent buoys in an approximate straight-line from a given pile or pile bent. In other words, if the first buoy was 20 m away, then the second buoy would be positioned at 40 m; the third at 80 m; the fourth at 160 m; and the fifth at 320 m. However, sometimes this "double-the-distance" rule of thumb was not used if doing so would have resulted in obstructions between the buoys and the pile or pile bent, or if a buoy was malfunctioning. Distances were approximated during deployment using a LaserWorks Long Distance 1200-Yard Hunting Rangefinder (LaserWorks, Wilder, KY) and were later verified using GPS coordinates from the on-board GPS units. Data collection locations relative to the piles are summarized in Table II along with water depth information from each site. Once buoys were positioned, hydrophones were hung from the buoys into the water at approximately half the water depth. Vertical alignment was maintained by attaching a 2-kg sinker to the end of each hydrophone cable. Raw data were sampled at a rate of 48 kHz. Note that data were collected both during pile driving and under ambient (i.e., no pile driving) conditions.

C. Data analysis

Single-strike sound-exposure levels (SELs), root-mean-squared (RMS) sound-levels, and maximum (PEAK) sound-levels were computed using the procedure described in detail by Madsen *et al.* (2006). As recommended, these quantities were computed in the pressure domain prior to conversion to dB using an algorithm where local peaks associated with blows or vibrational events were identified (The Mathworks, 2024). Because analysis was conducted in the pressure domain, it was easy to distinguish "drive event" from ambient noise, regular construction noise, etc., and signal-to-noise ratios (SNRs) were deemed to be a non-issue in the context of this analysis for the most part. SNRs were examined in dB using the furthest buoy from each drive. On average, across all sites, the SNR associated with the furthest buoy from each pile drive was 8.5 dB, and closer to the piles, SNRs were much greater than the 10 dB recommended by ISO (2017).

Least-squares best-fit regression was used to fit equations of the form

$$L_r = b - a\log_{10}\left(\frac{r}{r_0}\right), \tag{10}$$

to the data where a and b represent best-fit coefficients. In Eq. (10), a should correspond to A while b should correspond to $L_s - B$. In addition to this, 1/1 octave band analysis was conducted in the frequency domain whereby sound signals were filtered into each 1/1 octave bin, and equations of the form of Eq. (10) were fit to the data within each octave bin. Then, a and b from each octave bin were analyzed as a

TABLE II. Water depth, channel width (at the bridge), and Buoy position data relative to the piles at each site. N/A stands for "not applicable" and indicates that this buoy was not used for data collection; all data is in meters.

Site name	Water depth	Approximate channel width	Buoy 1	Buoy 2	Buoy 3	Buoy 4	Buoy 5
Bayway E	3.4	457	25	73	370	N/A	N/A
Dunn's Creek	6.8	101	60	202	396	N/A	N/A
Ribault River Drive 1	2.2	96	25	49	70	195	N/A
Ribault River Drives 2-4	2.2	96	27	50	107	200	N/A
Suwannee River	3.9	84	15	65	102	N/A	N/A
CR-218	3.0	50	53	82	124	191	235
SR-23 Drives 1-2	7.4	114	35	80	221	310	N/A
SR-23 Drives 3-9	7.4	114	38	97	196	257	348
Choctawhatchee Bay	4.5	49	14	44	78	139	176
Howard Frankland (West) Drives 1-8	7.0	4760	16	87	154	257	324
Howard Frankland (West) Drives 9-12	7.0	4760	18	128	175	275	N/A
Howard Frankland (West) Drives 13-18	7.0	4760	18	52	91	183	238
Howard Frankland King Piles Drives 1-2	4.3	4760	0.5	50	104	201	395
Howard Frankland King Piles Drives 3-11	4.3	4760	1	54	105	201	402
Howard Frankland (East) Drives 1-7	4.2	4760	18	42	106	207	400
Howard Frankland (East) Drives 8-15	4.2	4760	62	100	403	N/A	N/A
Simpson's Creek	1.9	20	49	93	145	N/A	N/A
Loxahatchee River	4.0	200	46	92	145	N/A	N/A
Manatee River	3.5	1340	53	121	209	N/A	N/A
NASA Causeway Drives 1-3	3.2	4360	15	50	200	300	N/A
NASA Causeway Drives 4-9	3.2	4360	49	204	405	N/A	N/A
Broward River	3.1	34	9	15	33	60	N/A

function of frequency. The result (see the following section) of this analysis was an apparent empirical model for L_r that appears to be frequency dependent. As such, investigators conducted a verification study using this new empirical model.

Two methods were used during verification: recreation of attenuation coefficients measured via regression using data from this study and using data from Buehler *et al.* (2015). During the former procedure, data from the buoy closest to the pile drives were used to model attenuation coefficients using a "blind" test. Due to the paucity of steel vibratory data, only steel impact and concrete impact data were used during this analysis. During this procedure, bulk quantities at each buoy (i.e., PEAK, RMS, and SEL) were computed for each drive and best-fit regression was used to characterize a as a function of r/r_0 for each drive. As will be discussed in the following, data suggested an apparent relationship between a and b, and as such, best-fit regression was used to develop a relationship between a and b using all data of a particular drive-type while excluding one data set. The apparent relationship between a and b was of the form

$$b = a_1 a + a_2, \tag{11}$$

where a_1 and a_2 represent best-fit coefficients. This process was repeated in a loop so that each dataset was sequentially replaced/used as the "blind" test for the model. As alluded to previously, model coefficients and "blind" tests were examined as a function of drive-type. In other words, steel impact driving led to different a_1 and a_2 coefficients than concrete impact driving, and as such, the steel impact coefficients were used to predict results from steel data sets, and the concrete impact drives were used to predict results from concrete data sets.

During the latter verification procedure, reported 10-m sound data from Buehler *et al.* (2015) were used in conjunction with equations of the form of Eq. (11) to predict the reported attenuation coefficient (i.e., A-values) reported by Buehler *et al.* (2015). In addition, an explicit analysis was conducted using data from the Choctawhatchee Bay Bridge.

During both verification scenarios, attenuation coefficients were plotted as a function of measured data and compared with both the $y = x$ line and best-fit regression lines of the form $y = a_{fit}x$ where a_{fit} represents the linear best-fit coefficient between data and modeled values for A.

III. RESULTS AND DISCUSSION

A. Results from field data

Results are summarized in Table III. Note that at some locations, a-values and b-values were relatively consistent with one another at a given site whereas at other locations, these best-fit coefficients varied significantly from drive-to-drive at the same site. However, investigators noted that even if a and b varied from drive-to-drive, they appeared to consistently be related to one another as shown in Fig. 1 regardless of drive-type (i.e., vibratory vs percussion), pile-type (i.e., concrete PCP, steel sheet, hollow steel, W-section), or hammer-type. Data appeared to indicate as well that because all these data were recorded throughout the state and geotechnical conditions varied from site-to-site, this relationship may be consistent across Florida geotechnical conditions.

As noted previously, in general, data appear to indicate a sort of "coupling" between a and b for the drives examined here that was consistently of the form of Eq. (11). When investigators filtered the PEAK sound-levels into octave frequency bins, similar relationships to Fig. 2 were observed in each frequency bin in the sense that within each frequency bin, b appeared to be a function of a (and vice versa), although the best-fit coefficients, a_1 and a_2 were different in each frequency bin. However, data suggested that a_1 and a_2 were related to one another as well. This result is summarized in Fig. 2.

As shown, results suggested that a_2 is a function of a_1 via a relationship of the form

TABLE III. Results summary table showing a-value and b-value ranges from each site; both a and b are in dB.

Site Name	a_{RMS}	b_{RMS}	a_{SEL}	b_{SEL}	a_{PEAK}	b_{PEAK}
Bayway E	14	163	14	16	6	161
Dunn's Creek	17	175	17	176	12	177
Ribault River	38–49	214–238	30–34	187–203	32–43	217–243
Suwannee River	33–36	232–241	22–25	202–209	26–29	235–242
County Road 218	25–46	193–227	30–34	199	38–46	230–243
State Road 23	17–30	174–209	17–28	175–203	10–26	180–221
Choctawhatchee Bay	51–61	224–265	51–59	224–264	47–54	229–266
Howard Frankland (West)	32–47	219–256	33–49	218–252	25–45	22–268
Howard Frankland King Piles	11–25	190–224	11–24	13–206	10–25	202–237
Howard Frankland (East)	6–54	13–278	7–40	171–238	7–42	200–267
Simpson's Creek	74	298	63	275	64	299
Loxahatchee River	26–44	199–232	25–36	19–214	30–47	226–256
Manatee River	20–32	180–211	20–32	182–212	20–33	197–223
NASA Causeway	5–43	147–228	6–40	152–253	7–47	174–255
Broward River	21	173	15	164	33	205

https://doi.org/10.1121/10.0034619

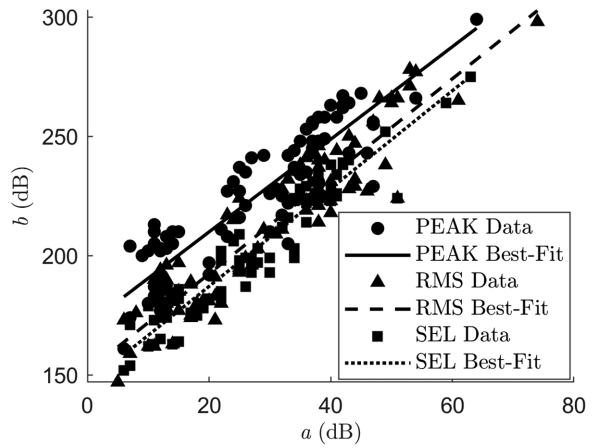

FIG. 1. Apparent relationships between a and b showing RMS, SEL, and PEAK data.

$$a_2 = a_3 a_1 + a_4, \tag{12}$$

where a_3 and a_4 are two more linear best-fit coefficients. Substituting Eqs. (11) and (12) into Eq. (10) and rearranging yields

$$L_r = a_4 + a_1(a_3 + a) - a\log_{10}\left(\frac{r}{r_0}\right). \tag{13}$$

Alternatively,

$$L_r = a\left[a_1 - \log_{10}\left(\frac{r}{r_0}\right)\right] + a_3 a_1 + a_4. \tag{14}$$

Note the interdependency among the attenuation terms is behaving exactly like the interdependency described by Ainslie *et al.* (2014) and described in Eqs. (4), (5), and (8).

Since a_1 (and a_2) are related to frequency, the second term in Eq. (13) may also be related to frequency. Alternatively, Eq. (14) implies that a is partially frequency dependent. While Eqs. (13) and (14) are similar to Eqs. (6) and (8), note that the "additional" term in Eqs. (6) and (8) is usually on the order of magnitude of dB/km whereas the "additional" frequency dependent attenuation in Eqs. (13) and (14) appears to be on the order of magnitude of dB/m and appears to be related to spreading loss associated with a.

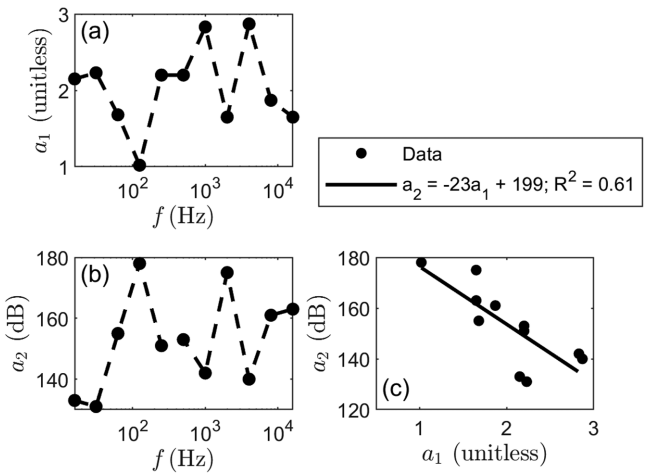

FIG. 2. Apparent frequency dependency between best-fit coefficients showing (a) a_1 as a function of frequency; (b) a_2 as a function of frequency; and (c) a_2 as a function of a_1.

Analysis of Table III shows that in general, at higher frequencies, attenuation appears to increase. In addition, data in Fig. 2 suggest that at very low frequencies (i.e., ~100–500 Hz or less, depending on the site), attenuation also appears to increase. According to the literature (see, for example, Jensen *et al.*, 2011, among many others), logarithmic decay equations for underwater sound attenuation in channels assume that all sound is produced above the cutoff frequency. The cutoff frequency, f_c, for each site was computed based upon each site's water depth using the following expression from Jensen *et al.* (2011):

$$f_c = \frac{C_w}{4D\sqrt{1 - \left(\frac{C_w}{C_b}\right)^2}}, \tag{15}$$

where c_w is the sound speed in water, c_b is the sound speed in the sediment, and D is the water depth of the channel. Values for c_b were estimated using surface sediment parameters reported by Rogers (1981) following Hamilton (1980). We understand that Eq. (15) is for an infinitely wide waveguide and the situations examined in this manuscript are all rivers and creeks with finite widths. However, as shown in Table II, these rivers and creeks were all very wide relative to their depths with a maximum depth-to-width ratio of 0.1, in the case of Simpson's Creek. As a result of this small depth-to-width ratio, investigators assumed that Eq. (15) was valid. But, based upon this assumption and the method used to estimate c_b, computed values for f_c (see Table IV) should be interpreted as order-of-magnitude approximations only.

As per Table IV, note that frequencies below ~100–500 Hz correspond approximately to the cutoff

TABLE IV. Water depth and cutoff frequency data from each drive.

Site name	f_c (Hz)	c_b (m/s)
Bayway E	295	1617
Dunn's Creek	125	1673
Ribault River	447	1620
Suwannee River	199	1718
County Road 218	283	1673
State Road 23	136	1617
Choctawhatchee Bay	221	1617
Howard Frankland (West)	97	1802
Howard Frankland King Piles	160	1802
Howard Frankland (East)	161	1802
Simpson's Creek	376	1750
Loxahatchee River	169	1802
Manatee River	193	1802
NASA Causeway	256	1718
Broward River	482	1550

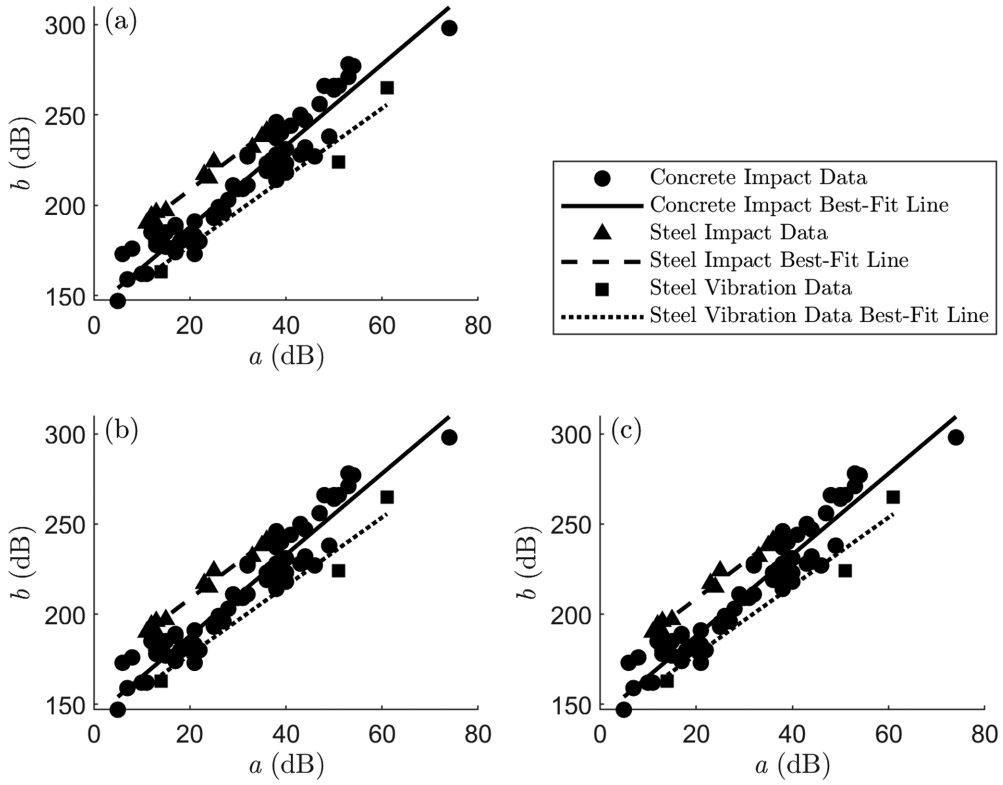

FIG. 3. Relationships between a and b sub-divided by drive-type showing (a) RMS data; (b) SEL data; and (c) PEAK data.

frequencies associated with water depths studied. These data suggest then that below the cutoff frequency, attenuation is very fast, but apparently not instantaneous. Data suggest that the empirical model presented in Eqs. (13) and (14) appears to capture this non-instantaneous decay as a function of distance associated with the pile drives studied in Florida.

Furthermore, investigators noted that there was some scatter in the data in Fig. 1 and hypothesized that this may be due to different drive-types (i.e., vibratory vs steel impact driving vs concrete impact driving). Investigators further subdivided Fig. 1 by drive-type as shown in Fig. 3. Note that in each case, a_1 was similar regardless of drive-type and was consistently close to 2.0. The differences in drive-type appear to manifest in differences in a_2 values, or alternatively a_3 values when referencing Eqs. (12)–(14). This would appear to indicate that a_2 is representing a psuedo-source term—i.e., some combination of strike energy, pile penetration, and drive-type, and this result is consistent with Martin and Barclay (2019).

A model was developed using the non-frequency-dependent version of the equations noted perviously [i.e., Eqs. (10) and (11)] in conjunction with Fig. 3. Substituting Eqs. (11) into Eq. (10),

$$L_r = (a_1 a + a_2) - a \log_{10}\left(\frac{r}{r_0}\right). \tag{16}$$

Best-fit coefficients associated with this model are summarized in Table V. If sound is known at one location, Eq. (16) and Table V may be used to solve for a which must correspond to A as per Eq. (10). Then, Eq. (10) may be used to compute L as a function of r. While the logic here appears to be somewhat circular, the result does agree with Ainslie *et al.* (2014) who pointed out that there should be interdependency among attenuation coefficients like this.

Please note that the model proposed previously inherently has some constraints in the sense that to use the model, sound must be known at one location, and the sound at this location must be greater than the a_2 coefficient associated with the drive-type in Table V. Explicitly, rearranging Eq. (16),

$$L_r - a_2 = a\left[a_1 - \log_{10}\left(\frac{r}{r_0}\right)\right]. \tag{17}$$

Thus, for the model to return, a valid value for a, L_r would have to be greater than the a_2 coefficient used when the model is applied. If the measured sound-level is lower than the a_2 coefficient, the model will yield nonsensical results in

TABLE V. Best-fit coefficients summarized by drive-type.

	Steel Vibration	Steel Impact	Concrete Impact
a_{1RMS}	1.9	2.2	2.1
a_{2RMS}	151.6	177.8	166.4
a_{1SEL}	1.9	2.5	2.2
a_{2SEL}	140	145.2	141.5
a_{1PEAK}	1.9	2.0	2.3
a_{2PEAK}	139.6	168.1	142.8

https://doi.org/10.1121/10.0034619

the sense that the model will predict that the sound gets louder as a function of distance, which of course, cannot be true. As such, to use the model presented here, it is critical that the initial sound-level used to start the computation is higher than its associated a_2 coefficient. Or, put another way, it would be best to "start" this model using a data source as close to a pile drive as possible where sound-levels are likely to be loudest.

B. Model verification

Three datasets were used to verify the new empirical *A*-value calibration model.

1. Data from this study

First, the "blind prediction" procedure described previously was conducted. Results of this analysis are presented in Fig. 4.

Please note that in Fig. 4, data where the closest sound-levels were lower than a site's a_2 coefficient were omitted from analysis because they would have produced nonsensical results. As shown, results were generally favorable in the sense that the new model was able to blindly predict *A*-values with a maximum average error ~10% (i.e., average $a_{fit} \sim 1.1$). Obviously, excluding one dataset per verification run produced slightly different a_1 and a_2 coefficients for each run. The maximum standard deviation associated with this for a_1 and a_2, respectively, was 0.05 and 0.93 dB with steel impact data and 0.02 and 0.45 dB with concrete impact data. Overall then, these results suggest small variability with the model as the model's fit coefficients were three orders of magnitude higher than their associated standard deviations.

2. Choctawhatchee Bay Bridge

Despite the paucity of steel vibratory data mentioned previously (i.e., only two sites with two sheets at each site), investigators sought to perform a true verification analysis on one of the bridges where sound data were measured during this study by comparing modeled data with data at the same location from some other source. Buehler *et al.* (2015) reported two datasets from the Choctawhatchee Bay Bridge where data were collected during impact pile driving. As shown in Table I, steel vibratory data were analyzed during this study at this location. As shown in Table III, during this study, *A*-values were estimated to be very high and ranged from 47 to 61 dB. However, Buehler *et al.* (2015) reported *A*-values that were much lower and that ranged between 13 and 25 dB. Thus, investigators attempted to determine if the new empirical model could help explain this apparent

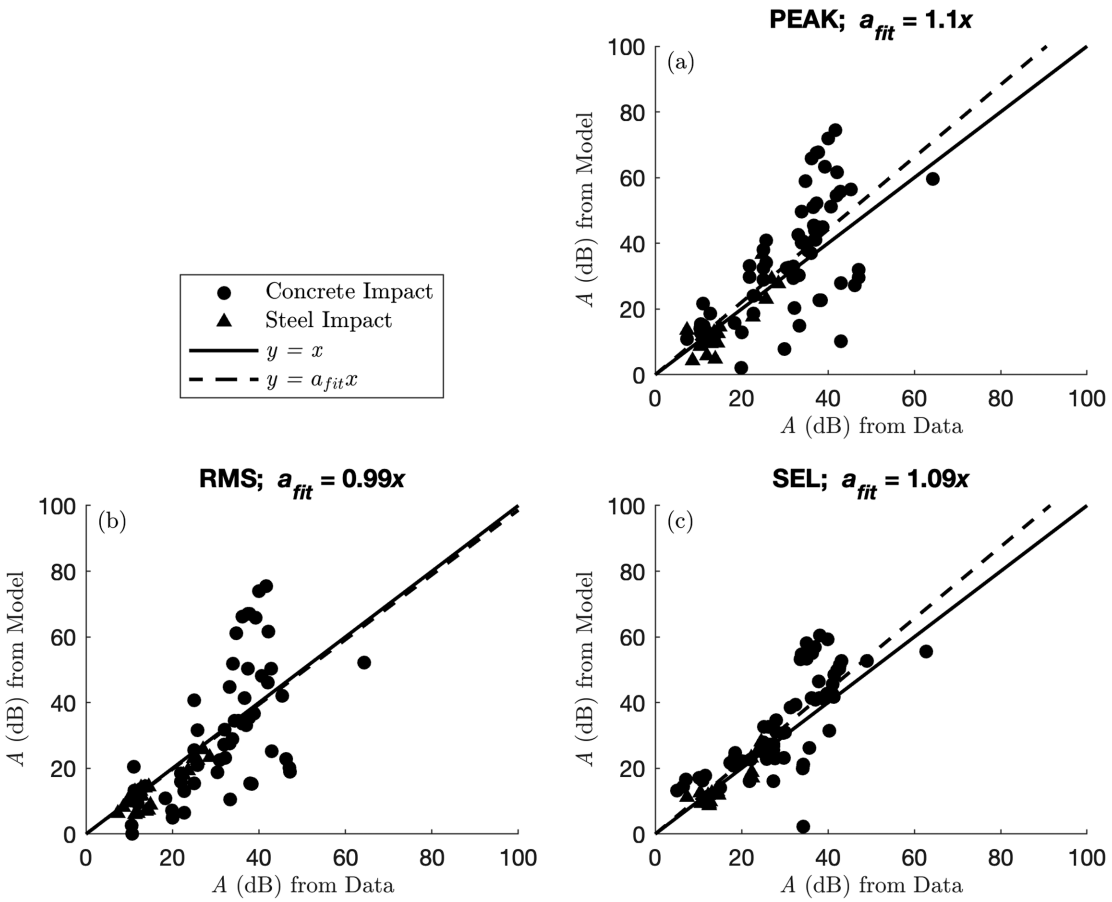

FIG. 4. *A*-values from the new empirical model using sound data closest to each pile drive compared to *A*-values obtained using best-fit regression showing results from (a) PEAK; (b) RMS; and (c) SEL.

discrepancy in attenuation as well as reproduce previous A-value data reported by Buehler *et al.* (2015) despite the noted possible deficiencies associated development of the models' vibratory a_1 and a_2 coefficients.

Choctawhatchee Bay Bridge data from Buehler *et al.* (2015), consisted of data from two categories of concrete piles. Both sets of concrete piles, dubbed type I and type II piles, were 76-cm square PCPs that were 48 m in length. The type II piles were solid throughout their lengths, whereas the type I piles only contained 3 m of solid sections near their tips while the balance of these piles were hollow.

A summary table showing modeled results and results from Buehler *et al.* (2015) is shown in Table VI. As shown, the new empirical model was able to reproduce the previously reported A-values relatively accurately despite the fact that different A-values (presumably resulting from different piles and associated noise sources) were measured during this study at the same location and that using the new model with vibratory data could be considered questionable due to the lack of data associated with the vibratory model's coefficients. To summarize, for type I piles, the new empirical model yielded A-values for PEAK, RMS, and SEL, respectively, on average of 21, 19, and 14 versus reported values of 16, 15, and 13. For type II piles, on average, application of the new empirical model resulted in A-values for PEAK, RMS, and SEL, respectively, of 27, 25, and 20. For these same data, reported values were 22, 20, and 20 respectively.

3. Non-Florida data

Next, analysis was conducted using non-Florida data by repeating the Choctawhatchee Bay procedure for computing A-values at each other site where Buehler *et al.* (2015) reported both A-values and 10-m sound data values. For details about the data used by Buehler *et al.* (2015), please refer to the summary table of the non-Florida data used for verification (see the Appendix). Alternatively, the reader is encouraged to consult Crowley and Gelsleichter (2023) for a detailed discussion of these data. The results of the comparison analysis are presented in Fig. 5.

While Fig. 5 shows general agreement between modeled and reported data, there is still some discrepancy between the results and the $y = x$ line. A new analysis was conducted whereby data from Buehler *et al.* (2015) that did not conform to the Florida data presented here was omitted. Specifically, data from the following instances were excluded from further analysis:

- Very large piles with diameters of 1.8 m or greater and very small piles with dimensions of 35 cm or less. These piles were either larger or smaller than the Florida piles studied here. This resulted in the omission of data from the Benicia-Martinez Bridge, Mad River Bridge, Schuyler Heim Bridge, Northern Rail Extension (all large piles), and the Noyo Harbor Dock (very small piles).
- Where reported A-values were based upon sound readings at only two locations because computing A based upon only two data points would not really be considered "regression" so much as "connecting two points with a logarithmic line." This resulted in the omission of data from Cleer Creek.
- Very shallow water (i.e., water depths of 1-m or less). This resulted in omission of additional data from the Northern Rail Extension.
- H-pile data because no H-piles were analyzed as part of this study. This resulted in the omission of data from the Hazel Bridge, Parson Slough, and Petalumia River Bridge.

After omitting these data, results were re-plotted (Fig. 6). As shown in Fig. 6, very close agreement between modeled data and reported data was achieved for RMS and PEAK. For SEL, discrepancies were observed, although in general, the new model was conservative in the sense that it tended to underpredict A. However, the procedure described by Madsen *et al.* (2006) is difficult from an algorithmic perspective in the sense that employing this method requires one to isolate each hammer blow, and depending on the algorithm used during this process, it is very easy to "miss" blows from time to time. While we are confident that we correctly isolated each blow, it is not possible to verify that all the authors from the data

TABLE VI. Choctawhatchee Bay Bridge verification summary table.

Pile ID	Pile type	A_{PEAK} reported (dB)	A_{PEAK} computed using new model (dB)	A_{RMS} reported (dB)	A_{RMS} computed using new model (dB)	A_{SEL} reported (dB)	A_{SEL} computed using new model (dB)
26	Type I	16	23	15	20	13	15
28	Type I	16	21	15	20	13	15
30	Type I	16	22	15	21	13	15
25	Type I	16	22	15	21	13	15
32	Type I	16	17	15	16	13	10
13	Type II	22	28	20	25	20	17
15	Type II	22	30	20	26	20	21
22	Type II	22	30	20	26	20	21
14	Type II	22	21	20	22	20	17
18	Type II	22	31	20	29	20	24
20	Type II	22	27	20	26	20	21
24	Type II	22	26	20	24	20	20

https://doi.org/10.1121/10.0034619

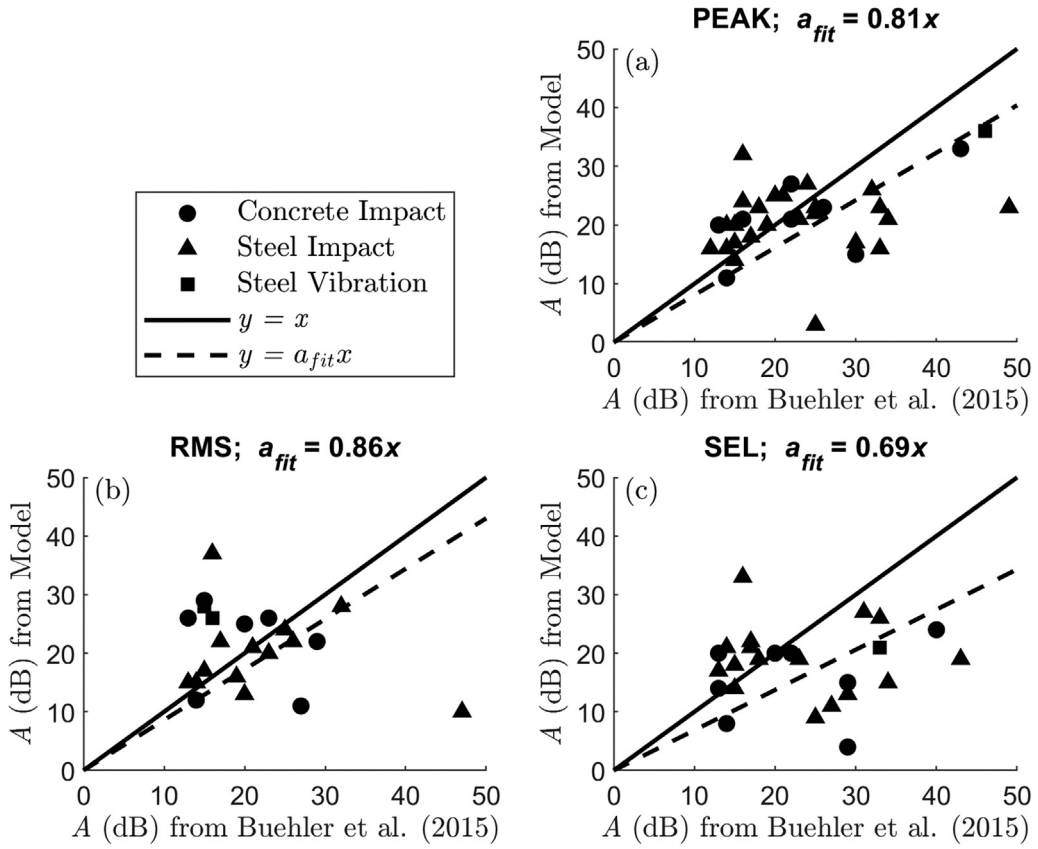

FIG. 5. *A*-values from the new empirical model computed using reported 10-m sound data as a function of *A*-values reported in the literature showing (a) PEAK; (b) RMS; and (c) SEL results.

reported by Buehler *et al.* (2015) similarly isolated each blow correctly, and this may explain the discrepancies seen in Fig. 6(c).

4. Model limitations

Data from the verification study appear to indicate that the model presented in this manuscript could be thought of as a calibrator for *A*-values under certain driving conditions. However, the authors of this paper suggest that this model be only applied under a very specific set of circumstances—specifically in instances where driving conditions are like driving conditions used to develop this model. These conditions are the following:

- Pile-type/drive type—we suggest that this model only be used as a calibration for square PCPs with dimensions between 46 cm wide and 91 cm wide or circular steel piles up to a maximum diameter of 168 cm, each driven using an impact hammer. For vibrational drives, we suggest only using the data presented here to calibrate *A* for 46-cm sheet piles or 61 cm steel circular piles due to the limited vibrational data studied here, if at all. However, based on model recreation performance, data suggest that vibrational drives are not necessarily this model's strength and the model should be used cautiously (or maybe not at all) in these situations. On the steel impact side of the equation, The model may be used for W40x183 piles specifically because so many were studied here but extending this model to other wide-flange sections would appear to be questionable—especially because H-piles consistently performed poorly when compared to this model. Overall, investigators are of the opinion that this model's best application is for concrete piles of certain dimensions driven via impact driving. While this would appear to be a limited set of scenarios, such drives constitute the vast majority of pile drives in Florida transportation projects.
- Water depths—we note that all the data presented herein was in relatively shallow channels with depths between 2 and 15 m. This is typical of pile driving in Florida. Extending this model to deeper water would appear to be incorrect, however.

In addition to this, another limitation of this model is associated with its application and was noted previously in the sense that the sound data used to "start" the model must be higher than the drive-type's associated a_2 coefficient or else the model will yield a nonsensical result. As stated previously, this implies that the data used to "start" the model should be taken as close to the pile drive as possible where sound levels are likely to be the loudest.

While these limitations are important to point out, the model presented here may be a useful design tool—particularly in the State of Florida where, in conversations with the Florida Department of Transportation (FDOT), as

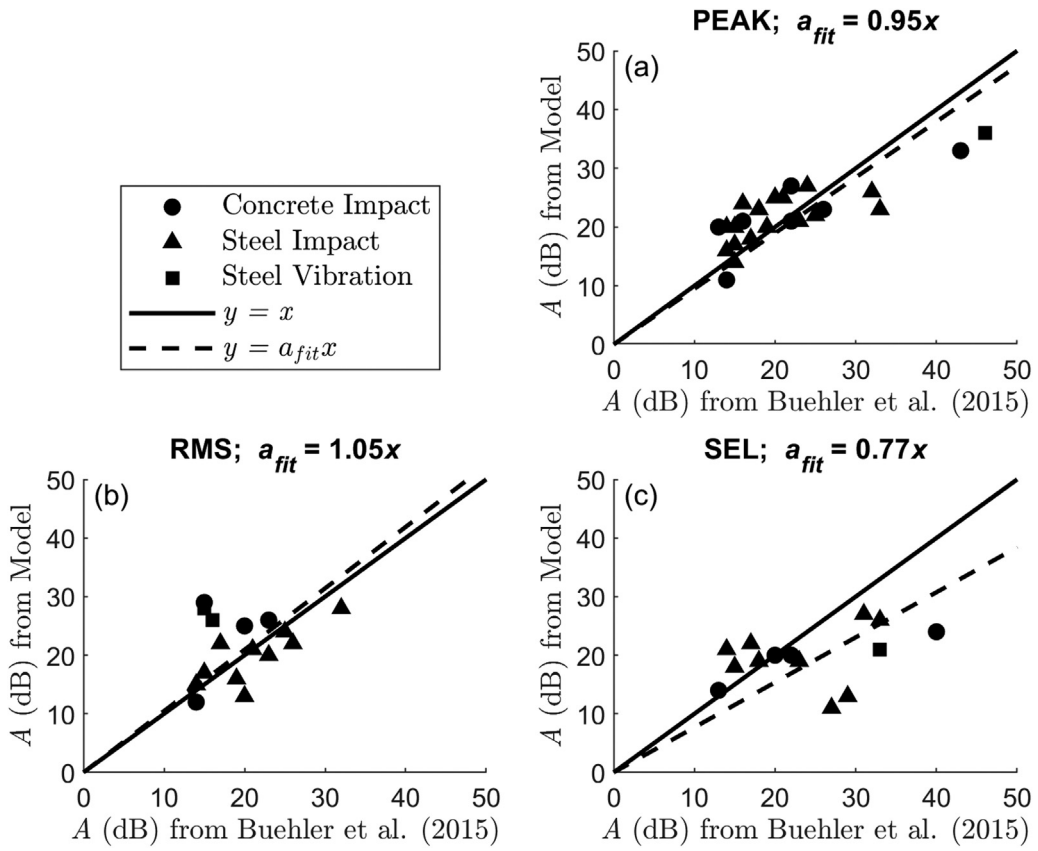

FIG. 6. *A*-values from new model computed using 10-m sound data reported by Buehler *et al.* (2015) as a function of *A*-values reported by Buehler *et al.* (2015) using only data conforming to the Florida data collected during this study showing (a) PEAK data; (b) RMS data; and (c) SEL data.

mentioned previously, it was discussed that the vast majority of transportation-related pile drives in the state that would result in underwater pile driving noise is in relatively shallow channels with piles that range between 46 and 92 cm in diameter. Since FDOT conducts so many drives with these types of piles, applying this model to that sort of repeating scenario may prove useful.

5. Implications of the new model

Results here are encouraging, but admittedly, it remains counterintuitive to the authors why there is an apparent "link" between a pseudo-source term (i.e., b) and attenuation (i.e., a or A). The frequency analysis presented previously is an attempt to provide a possible explanation in the sense that this "link" appears to manifest in some sort of frequency dependency, but the authors are aware that this is less so a physical explanation and more simply a regression showing apparent dependencies that were observed in the data.

At present, the best clues about a more physical explanation about why the empirical model presented here appears to show the apparent "link" between source and attenuation may be hypothesized by combining results from this study with previous data from Martin and Barclay (2019) who recognized that strike energy and pile penetration tend to dictate the source term (or pseudo-source term), at least to some extent. In the present study's regression analysis, these strike energy and pile penetration terms would tend to be lumped into b along with the other source or pseudo-source terms from Eq. (9) and the water-column attenuation term (i.e., the α term) which is expected to be small, relatively speaking and is typically reported to be on the order of dB/km. In Fig. 2 and Eqs. (11)–(14), an apparent frequency dependency is shown for attenuation. Taken together, these results imply that similarly, pile penetration and strike energy may be functions of frequency in the sense that different strike energies or pile penetration depths (or both) result in source-levels with different frequencies that are then attenuated at different rates. However, this hypothesis requires additional research and at this point is merely a hypothesis.

IV. SUMMARY AND CONCLUSIONS

To summarize:

- Underwater pile driving noise data from Florida were collected from 84 pile drives across 15 pile driving scenarios in the state. Best-fit regression was used to infer *A*-values for each of these pile drives. In each case, sound attenuation was governed by a well-known logarithmic regression equation of the form $L_r = b + a\log_{10}(r/r_0)$.
- Investigators noted that a and b appeared to be linearly correlated to one another, and as such, a model was

https://doi.org/10.1121/10.0034619

developed to infer a (which should correspond to A) if sound is known at one location.
- Further analysis appeared to indicate that this empirical calibration of A, which may sometimes result in very high values for attenuation, may be the result of very fast, but apparently non-instantaneous attenuation near and/or below the cutoff frequency.
- A verification study was conducted, and results appeared to show that the empirical calibration presented here is capable of reproducing data from other sources under very specific circumstances—specifically for pile-types, water depths, and drive-types similar to the conditions studied here.

The calibration model presented here for A (again, under very specific conditions) may be a useful design tool for investigators conducting pile driving under similar conditions to the conditions examined during this study—especially for concrete piles in shallow water depths driven via impact hammers. While this may be true, additional research should be conducted regarding the apparent "link" between this model's source term and attenuation so a more physically based model for attenuation in these sorts of piles may be developed.

ACKNOWLEDGMENTS

The authors of this paper wish to thank the FDOT for their support of this research—particularly Katasha Cornwell and Rodrigo Herrera, PE. Special thanks as well to Denise Rach (FDOT), Nicole Cribbs (Faller Davis), Jason Russel (FDOT), Ted Devens (Stantec), and Jason Russell (FDOT) for their commentary throughout this project. This work was funded by FDOT Contract No. BDV34-985-03, Katasha Cornwell, Project Manager.

AUTHOR DECLARATIONS

Conflict of Interest

The authors have no conflicts of interest to disclose.

DATA AVAILABILITY

The data that support the findings of this study are available from the corresponding author upon reasonable request.

APPENDIX

See Table VII for data used for verification.

TABLE VII. Summary of data used for verification. Data in italics were excluded from Fig. 6.

Site name	Site location	Drive type	Pile type
Norfolk Naval Station	Norfolk, VA	Concrete impact	61 cm square PCP
Noyo Harbor Dock	*Fort Bragg, CA*	*Concrete impact*	*36 cm square PCP*
Kawaihae Harbor	Kawaihae, HI	Concrete impact	42 cm oct. PCP
Shell Martinez Refinery	Martinez, CA	Concrete impact	61 cm square PCP
Humboldt Aquatic Ctr.	Eureka, CA	Concrete impact	61 cm oct. PCP
Berth 22, Oakland, CA	Oakland, CA	Concrete impact	61 cm square PCP
Northern Rail Extension	Salcha, AK	Steel vibration	61 cm steel shell
Naval Base Kitsap	Bangor, WA	Steel vibration	61 cm steel shell
Naval Base Kitsap	Bangor, WA	Steel vibration	61 cm steel shell
Benicia-Martinez Bridge	Benicia, CA	Steel impact	244 cm CISS pipe
Richmond/San Rafael Fenders	San Fransisco, CA	Steel impact	36 cm steel pipe
Airport Rd. Bridge	Sacramento, CA	Steel impact	41 cm steel pipe
Bradshaw Bridge	Lathrop, CA	Steel impact	51 cm steel pipe
Tongue Point Pier	Astoria, CA	Steel impact	61 cm steel pipe
Cleer Creek WWTP	*Redding, CA*	*Steel impact*	*61 cm steel pipe*
Portland-Milwaukie Lt. Rail	Portland, OR	Steel impact	61 cm steel pipe
SR-520 Test Pile	Seattle, WA	Steel impact	76 cm steel pipe
Noyo Bridge	Fort Bragg, CA	Steel impact	152 cm steel pipe
Russian River Bridge	Ukiah, CA	Steel impact	168 cm steel pipe
Mad River Bridge	*McKinleyville, CA*	*Steel impact*	*221 cm steel pipe*
Hazel Bridge	*Sacramento, CA*	*Steel impact*	*H-pile*
Parson Slough	*Monterey, CA*	*Steel impact*	*H-pile*
Schuyler Heim Bridge	Long Beach, CA	Steel impact	61 cm steel shell
Schuyler Heim Bridge	Long Beach, CA	Steel impact	366 cm steel shell
Northern Rail Extension	Salcha, AK	Steel impact	61 cm steel shell
Northern Rail Extension	Salcha, AK	Steel impact	183 cm steel shell
Naval Base Kitsap	Bangor, WA	Steel impact	61 cm steel shell
Naval Base Kitsap	Bangor, WA	Steel impact	91 cm steel shell
Crescent City Inner Harbor	Cresent City, CA	Steel impact	61 cm steel shell
Coliseum Way Bridge	Oakland, CA	Steel impact	91 cm steel shell
Petaluma River Bridge	*Petaluma, CA*	*Steel impact*	*H-pile*
Port of Coeyman	Coeyman, NY	Steel impact	61 cm steel pipe

Ainslie, M. A. (**2010**). *Principles of Sonar Performance Modeling* (Springer, New York).
Ainslie, M. A., Dahl, P. E., de Jong, W. M., and Laws, R. M. (**2014**). "Practical spreading laws: The snakes and ladders of underwater acoustics," in *Proceedings of the 2nd International Conference and Exhibition on Underwater Acoustics*, June 22–27, Rhodes, Greece, pp. 879–886.
Bailey, H., Senior, B., Simmons, D., Rusin, J., Picken, G., and Thompson, P. M. (**2010**). "Assessing underwater noise levels during pile-driving at an offshore windfarm and its potential effects on marine mammals," Mar. Pollut. Bull. **60**, 888–897.
Brandt, M., Diederichs, A., Betke, K., Matuschek, R., and Nehls, G. (**2011**). "Responses of harbour porpoises to pile driving at the Horns Rev II offshore wind farm in the Danish North Sea," Mar. Ecol. Prog. Ser. **421**, 205–216.
Buehler, D., Oestman, R., Reyff, J., Pommerenck, K., and Mitchell, B. (**2015**). *Technical Guidance for Assessment and Mitigation of the Hydroacoustic Effects of Pile Driving on Fish* (California Department of Transportation, Sacramento, CA).
Crowley, R., Berube, J., Matemu, C., Morgan, C., Kopp, B. T., Kernan, M., Dally, W. R., and Gelsleichter, J. J. (**2020**). "Development of a unique instrumentation system to monitor underwater noise due to pile driving," in *Proceedings of Geo-Congress 2020*, February 25–28, Minneapolis, MN, pp. 798–807.
Crowley, R., and Gelsleichter, J. J. (**2023**). *Underwater Noise Level Study During Impact Pile Driving* (Florida Department of Transportation, Tallahassee, FL), p. 712.
Dahl, P. E., Dall-Osto, D. R., and Farrell, D. M. (**2015**). "The underwater sound field from vibratory pile driving," J. Acoust. Soc. Am. **137**, 3544–3554.
Dahl, P. H., and Dall'Osto, D. R. (**2017**). "On the underwater sound field from impact pile driving: Arrival structure, precursor arrivals, and energy streamlines," J. Acoust. Soc. Am. **142**, 1141–1155.
Dahl, P. H., and Reinhall, P. G. (**2013**). "Beam forming of the underwater sound field from impact pile driving," J. Acoust. Soc. Am. **134**, EL1-EL6.
Dähne, M., Gilles, A., Lucke, K., Peschko, V., Adler, S., Krügel, K., Sundermeyer, J., and Siebert, U. (**2013**). "Effects of pile-driving on harbour porpoises (*Phocoena phocoena*) at the first offshore wind farm in Germany," Environ. Res. Lett. **8**, 025002.
Erbe, C., Reichmuth, C., Cunningham, K., Lucke, K., and Dooling, R. (**2016**). "Communication masking in marine mammals: A review and research strategy," Mar. Pollut. Bull. **103**, 15–38.
Finneran, J. J. (**2015**). "Noise-induced hearing loss in marine mammals: A review of temporary threshold shift studies from 1996 to 2015," J. Acoust. Soc. Am. **138**, 1702–1726.
Finneran, J. J., Trickey, J. S., Branstetter, B. K., Schlundt, C. E., and Jenkins, K. (**2011**). "Auditory effects of multiple underwater impulses on bottlenose dolphins (*Tursiops truncatus*)," J. Acoust. Soc. Am. **130**, 2561.
Hamilton, E. L. (**1980**). "Geoacoustic modeling of the sea floor," J. Acoust. Soc. Am. **68**, 1313–1340.
ISO (**2017**). ISO 18406:2017, "Underwater acoustics – Measurement of radiated underwater sound from percussive pile driving" (International Organization for Standardization, Geneva, Switzerland).
Jensen, F. B., Kuperman, W. A., Porter, M. B., and Schmidt, H. (**2011**). *Comptuational Ocean Acoustics* (Springer, London).
Jestel, J., von Pein, J., Lippert, T., and von Estorff, O. (**2021**). "Damped cylindrical spreading model: Estimation of mitigated pile driving noise levels," Appl. Acoust. **184**, 108350.
Kaczkowski, S. V. (**2010**). "Applications of model approximations to attenuation properties in sandy-silty sediments," in *Mathematics* (Rensselaer Polytechnical Institute, Troy, NY).
Kastelein, R. A., Helder-Hoek, L., Voorde, S. V. D., Benda-Beckmann, A. M. V., Lam, F.-P. A., Jansen, E., Jong, C. A. F. D., and Ainslie, M. A. (**2017**). "Temporary hearing threshold shift in a harbor porpoise (*Phocoena phocoena*) after exposure to multiple airgun sounds," J. Acoust. Soc. Am. **142**, 2430–2442.
Lippert, T., Ainslie, M. A., and von Estorff, O. (**2018**). "Pile driving acoustics made simple: Damped cylindrical spreading model," J. Acoust. Soc. Am. **143**, 310–317.
Lippert, T., Galindo-Romero, M., Gavrilov, A. N., and von Estorff, O. (**2015**). "Empirical estimation of peak pressure level from sound exposure level. Part II: Offshore impact pile driving noise," J. Acoust. Soc. Am. **138**, EL287–EL292.
Lippert, S., Nijhof, M., Lippert, T., Wilkes, D., Gavrilov, A., Heitmann, K., Ruhnau, M., von Estorff, O., Schäfke, A., Schäfer, I., Ehrlich, J., MacGillivray, A., Park, J., Seong, W., Ainslie, M. A., Jong, C. D., Wood, M., Wang, L., and Theobald, P. (**2016**). "COMPILE—A generic benchmark case for predictions of marine pile-driving noise," IEEE J. Oceanic Eng. **41**, 1061–1071.
Lippert, T., and von Estorff, O. (**2014**). "The significance of parameter uncertainties for the prediction of offshore pile driving noise," J. Acoust. Soc. Am. **136**, 2463–2471.
Lucke, K., Scowcroft, G., Winter, H. V., Knowlton, C., Lam, F.-P. A., Hawkins, A., and Popper, A. N. (**2016**). "International harmonization of approaches to define underwater noise exposure criteria and needs of the international regulatory community," Proc. Mtgs. Acoust. **27**, 070010.
MacGillivray, A. O. (**2013**). "A model for underwater sound levels generated by marine impact pile driving," J. Acoust. Soc. Am. **134**, 4024.
Madsen, P. T., Johnson, M., Miller, P. J., Aguilar Soto, N., Lynch, J., and Tyack, P. (**2006**). "Quantitative measures of air-gun pulses recorded on sperm whales (*Physeter macrocephalus*) using acoustic tags during controlled exposure experiments," J. Acoust. Soc. Am. **120**, 2366–2379.
Martin, S. B., and Barclay, D. R. (**2019**). "Determining the dependence of marine pile driving sound levels on strike energy, pile penetration, and propagation effects using a linear mixed model based on damped cylindrical spreading," J. Acoust. Soc. Am. **146**, 109–121.
NOAA (**2021**). *Section 7 Consultation Guidance How to Develop ESA Section 7 Consultation Requests* (National Oceanic and Atmospheric Administration, US Department of Commerce, Washington, DC).
Popper, A. N., and Hawkins, A. D. (**2019**). "An overview of fish bioacoustics and the impacts of anthropogenic sounds on fishes," J. Fish Biol. **94**, 692–713.
Reinhall, P. G., and Dahl, P. H. (**2011a**). "An investigation of underwater sound propogation from pile driving," in *WSDOT Research Report* (Washington State Department of Transportation, Office of Research and Library Services, Olympia, WA).
Reinhall, P. G., and Dahl, P. H. (**2011b**). "Underwater Mach wave radiation from impact pile driving: Theory and observation," J. Acoust. Soc. Am. **130**, 1209–1216.
Reinhall, P. G., Dardis, T., and Dahl, P. H. (**2015**). *Underwater Noise Reduction of Marine Pile Driving Using a Double Pile* (Washington State Transportation Center, Seattle, WA).
Rogers, P. H. (**1981**). *Onboard Prediction of Propogation Loss in Shallow Water* (Naval Research Lab, Washington, DC).
The Mathworks (**2024**). *MATLAB Version 2024a* (The Mathworks Inc., Natick, MA).
Tougaard, J., Wright, A. J., and Madsen, P. T. (**2015**). "Cetacean noise criteria revisited in the light of proposed exposure limits for harbour porpoises," Mar. Pollut. Bull. **90**, 196–208.
von Pein, J., Lippert, T., Lippert, S., and von Estorff, O. (**2022**). "Scaling laws for unmitigated pile driving: Dependence of underwater noise on strike energy, pile diameter, ram weight, and water depth," Appl. Acoust. **198**, 108986.
Weston, D. E. (**1971**). "Intensity-range relations in oceanographic acoustics'," J. Sound Vib. **18**, 271–287.
Weston, D. E. (**1994**). "Wave shifts, beam shifts, and their role in modal and adiabatic propagation," J. Acoust. Soc. Am. **96**, 406–416.
Wilkes, D. R., and Gavrilov, A. N. (**2017**). "Sound radiation from impact-driven raked piles," J. Acoust. Soc. Am. **142**, 1–11.